



# Maritime Technology and Research

<https://so04.tci-thaijo.org/index.php/MTR>



Research Article

## A novel ship path following method in inland waterways based on adaptive feedforward PID control

Siwei Xin<sup>1</sup>, Yixiong He<sup>1,2</sup> and Liwen Huang<sup>1,2,\*</sup>

<sup>1</sup>School of Navigation, Wuhan University of Technology, Wuhan 430063, China

<sup>2</sup>Hubei Key Laboratory of Inland Shipping Technology, Wuhan 430063, China

### Article information

Received: June 17, 2021

Revised: July 20, 2021

Accepted: July 27, 2021

### Keywords

Ship path following,  
Adaptive feedforward PID,  
Lead compensator,  
Course keeping,  
Nomoto model

### Abstract

Given the complex and time-varying external disturbances of inland waterways, designing an accurate path following controller is challenging. Based on the traditional PID controller, combined with the servo system model and the lead compensator, an adaptive feedforward PID controller for path following of ships in inland waterways is designed, considering ship maneuverability and external disturbances. Simulations of a ship in a curved channel in different scenarios are carried out to illustrate the effectiveness of the proposed path following method. Compared with the traditional path following controller, the proposed one, based on adaptive feedforward PID control, has favorable relative stability, anti-interference ability, and high steady-state precision in inland waterways.

## 1. Introduction

The navigational environment in inland waterways is complex, as the sediment movement at the bottom is frequent, and the vertical and horizontal velocity changes significantly, which makes it difficult for ships to maneuver and increases navigation risks. Therefore, the establishment of an accurate ship path following controller is of great significance, in order to ensure the safe navigation of ships in inland waterways with complex navigational environments.

As the key and core of ship intelligent control, ship path following control has been of wide concern in recent decades. Especially, for long-distance navigation, path following with good control performance can reduce the labor intensity of seamen and improve operational efficiency, which can increase the safety of navigation (Zhang & Zhang, 2014; Fossen, 2011). With the prosperity of control theory, various advanced control strategies have been applied to the design of ship track-keeping controller. Track-keeping control for ships can be divided into path following control and trajectory tracking control (Boxu & Zhang, 2021). In this paper, we emphasize path following control, where the target track is time-independent. Due to their nonlinear and time-delay characteristics, path following control of ships is a highly nonlinear control process. This makes the design of an accurate path following controller challenging.

In recent years, a large number of algorithms and methods have been proposed for path following controllers for marine surface ships. Do et al. (2004) developed a nonlinear robust adaptive control strategy to force an underactuated surface ship to follow a predefined path at a

\*Corresponding author: School of Navigation, Wuhan University of Technology, Wuhan 430063, China  
E-mail address: [lw Huang@whut.edu.cn](mailto:lw Huang@whut.edu.cn)

desired speed. Do et al. (2004) developed state-feedback and output-feedback controllers that force an underactuated surface ship to follow a predefined path under the presence of environmental disturbances. Brevik et al. (2004) addressed the problem of path following for marine surface vessels by utilizing a novel guidance-based approach. Moreira et al. (2007) presented a path following control system for a surface vessel with particular reference to a possible future application to the Esso Osaka tanker. Borhaug et al. (2008) considered that using a modified Line-of-Sight (LOS) guidance law with integral action and a pair of adaptive feedback controllers for global asymptotic path following of straight-line paths. Furthermore, this paper showed an LOS decision variable can be incorporated into the MPC (Model Predictive Control) design to improve path following performance. Borhaug et al. (2011) proposed a decentralized controller based on a cross-track control law and a nonlinear synchronization control law, which can make the ship form a desired formation asymptotically along a given straight line path with a given forward speed profile. Bhattacharyya and Gupta (2014) proposed a trajectory control algorithm, termed “Target Path Iteration (TPI) algorithm”. Do (2016) used the backstepping method to design a robust adaptive path-following controller. Deng et al. (2019) designed a path following controller for a sail-assisted ship, and an adaptive fuzzy control law for such a ship was developed under the skeleton of LOS guidance. Wen et al. (2020) designed a ship path-following controller based on the characteristic model, which was convenient to use to adjust the controller structure as the navigation environment changed.

A nonlinear model-based controller is designed for a fully-actuated vessel to enable it to comply with the guidance commands. Liu et al. (2016) considered interrelated problems concerning the path following of marine surface vehicles, and neural network (NN) with iterative updating laws based on prediction errors were proposed to identify the dynamical uncertainty and time-varying ocean disturbances.

However, most research considered scenarios of shipping in open water with environmental disturbances, including those caused by wave, wind, and ocean-current. Cheng et al. (2019) studied ship track control in bridge areas based on the differential evolution algorithm. In inland waterways, the complex navigation environment, such as narrow waters, and a rapidly-changing flow, makes path following more difficult than in open water. Therefore, investigating the ship adaptive path following control in a curved channel of an inland waterway has an important application value.

As a common controller, PID has been widely used in ship autopilots because of the simple algorithm, good robustness, and high reliability. Moreover, PID controllers have been proposed for ship maneuvering motion simulation and path following control in different scenarios. Due to the complexity of PID parameter tuning, it is difficult to achieve the foremost control effect. To solve this problem, the genetic algorithm, the ant colony algorithm, and the particle swarm optimization algorithm are introduced to tune the parameters autonomously.

Sun et al. (2017) used the genetic algorithm to optimize PID parameters to achieve feedback control and ensure the stability of a system. CMAC neural network was used to realize feed-forward nonlinear control and ensure satisfactory control accuracy and system response speed. Feng and Bin (2018) combined traditional PID and the BP (Back propagation) neural network; the controlled object was identified by the BP neural network, the PID control parameters were given, and the PID control algorithm was used to control and optimize the convergence speed. A self-tuning PID algorithm course controller, based on the BP neural network, was designed.

The neural network algorithm has also been used to adjust parameters. Liu et al. (2002) designed a PID control combined with the Radial Basis Function (RBF) neural network for course control of ship steering. Zhan (2003) discussed the neural network control of PID parameter self-adjustment, which can automatically adjust PID parameters according to ship dynamic features, and through the ability of the neural network to approximate arbitrary nonlinearity to adjust 3 parameters, so as to overcome the impact due to model uncertainty and disturbance. Format (2014)

presented a nonlinear controller design by combining a neural network (NN) approximator with adaptive Backstepping technology.

Concerning the colony algorithm, Tomera (2014) described the application of an ant algorithm to optimize parameters of the ship course controller, based on the algorithm of PID control.

Cheng and Hong (2012) proposed an approach based on the artificial fish swarm algorithm (AFSA). Kouassi et al. (2020) proposed a novel tuning method based on the development of the standard particle swarm optimization (PSO) for optimum design of a fuzzy PID controller for a multivariable system; the parameters of membership functions and PID gains were optimized by modified PSO.

The particle swarm optimization algorithm has also been used to adjust parameters. Li et al. (2019) proposed a sliding mode variable structure PID control strategy, based on particle swarm optimization. Taking an actual track and course on the ground as the controlled object, the segmentation function was designed to modify the track deviation and limit the maximum and minimum.

Fuzzy rules have been used to adjust 3 parameters of a PID controller online. Cheng et al. (2018) proposed an improved genetic algorithm (GA), based on fuzzy rules, quantization factor, and scaling factor. He et al. (2011) developed a Fuzzy-PID controller based on the mathematical control model of a rolling mill, and used genetic algorithm for global optimization. Tomera (2017) used the classical linear control theory and the placement method to calculate the initial values of PID gains. A PID controller was synthesized using the Nomoto model of ship dynamics, identified on the basis of standard Kempf's zigzag maneuver and the Ant Colony Optimization algorithm (ACO).

However, the above research methods needed the prior information of parameters, which cannot guarantee the relative stability of a system and cannot meet the accuracy requirements of shipping in complex inland waterways. Therefore, this paper proposes an adaptive feedforward PID controller for path following of ships in inland waterways. The traditional PID controller is improved with a servo system model and a lead compensator for stability, anti-interference ability, and high steady-state precision.

The remainder of this paper is arranged as follows: Section 2 presents the maneuvering model of ships. Section 3 shows the design of the proposed feedforward PID controller. In Section 4, simulation of a ship in a curved channel is carried out to illustrate the effectiveness of the path following based on the adaptive feedforward controller. Section 5 concludes the main findings of this paper.

## 2. Modeling of ships and inland navigation environment

### 2.1 Maneuvering model of a ship

In research on the motion control of ships, transfer functions are frequently used. The most popular one is the Nomoto model, including the first-order linear KT equation and second-order linear KT equation. In a practical ship maneuvering system, the nonlinear feature of steering servo mechanisms has an unneglectable influence on path following effectiveness. Hence, the steering gear servo system is introduced in simulations (Zhang et al., 2019).

#### 2.1.1 The steering gear servo system

After receiving the command rudder angle  $\delta_r$ , the steering gear cannot obtain the required rudder angle immediately. A steering process with nonlinear saturation characteristics is needed. In the simulation system, the process should be considered, and a mathematical model should be established for the steering gear servo system (Yang et al., 2011; Velagic & Vukić, 2004; Velagic et al., 2003). The dynamic characteristics of the steering gear servo system are expressed as:

$$T_r \dot{\delta} + \delta = K_r \delta_r \quad (1)$$

where  $T_r$  is the time constant of the steering gear,  $K_r$  is the control gain of the steering gear,  $\delta_r$  is the command rudder angle,  $\delta$  is the actual output rudder angle, and  $\dot{\delta}$  is steering speed. Making conclusions from the present researches of Witkowska et al. (2007), Witkowska and Smierzchalski (2007), Witkowska and Smierzchalski (2009), and Dyda et al. (2019), the model can be simplified, as per **Figure 1**.

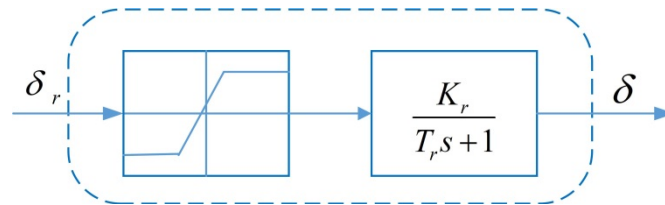


**Figure 1** Steering gear servo system.

Therefore, the transfer function  $W(s)$  of the steering gear servo system is as follows:

$$W(s) = \frac{\delta(s)}{\delta_r(s)} = \frac{K_r}{T_r s + 1} \quad (2)$$

where  $W(s)$  is transfer function,  $\delta(s)$  is the output (actual rudder angle), and  $\delta_r(s)$  is the input (command rudder angle). The pure lag characteristics of the steering gear should be fully considered in the modeling. Besides certain restrictions on rudder angle  $-35^\circ \leq \delta \leq 35^\circ$  and steering speed  $-3^\circ/s \leq \dot{\delta} \leq 3^\circ/s$ , the 2 correlation coefficients  $K_r$  and  $T_r$  should also be fully considered, to ensure the speed and control flexibility of the steering gear. The parameter values for the steering gear servo system are:  $K_r = 1s^{-1}$ ,  $T_r = 3s$ .

### 2.2 Nomoto model

In order to obtain the ship model, it is assumed that the ship is moving at constant speed in restricted calm water. Ship dynamics are obtained by applying Newton's laws. There are 6 directions of ship motion, since 6 independent coordinates are necessary to determine the spatial position and orientation of a rigid body. The 6 different motion components are: surge, sway, heave, roll, pitch, and yaw (Velagic et al., 2003). Accordingly, the most generally-used notation for these quantities is  $x, y, z, \varphi, \theta, \psi$ .

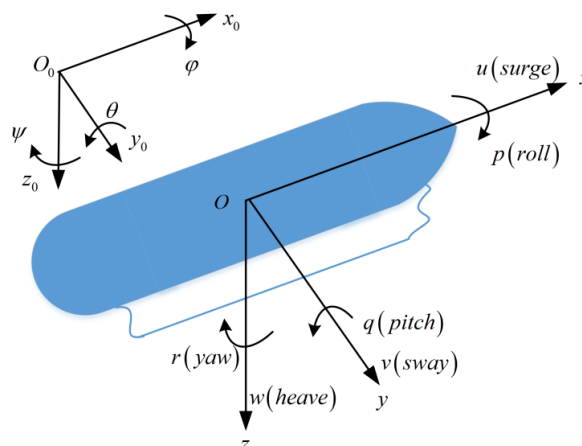


**Figure 2** Body- and earth-fixed reference frames.

**Figure 2** shows 6-coordinate definitions and a generally-adopted reference frame. The position and orientation of the ship are described relative to the earth-fixed reference frame  $O_0 - x_0y_0z_0$ .  $O_0x_0$  points to north,  $O_0y_0$  points to east, and  $O_0z_0$  points to the center of the earth.  $O - xyz$  is a body-fitted coordinate system.  $Ox$  points to the bow,  $Oy$  points to the starboard, and  $Oz$  points to the bilge keel. The general ship equations of motion can be expressed in compact form as:

$$M\dot{v} + c(v)v = \tau \tag{3}$$

where  $M$  is the inertia matrix,  $c(v)$  is the matrix of Coriolis and centripetal term,  $v = [u, v, w, p, t, r]^T$  is the ship linear and angular velocities vector, and  $\tau = [X, Y, Z, K, M, N]^T$  is a generalized vector of external forces and moments.

For course keeping and path following problems, only the horizontal-plane ship motion is used (**Figure 3**). Due to this, the 6DOF model is simplified and reduced to a 3DOF model.

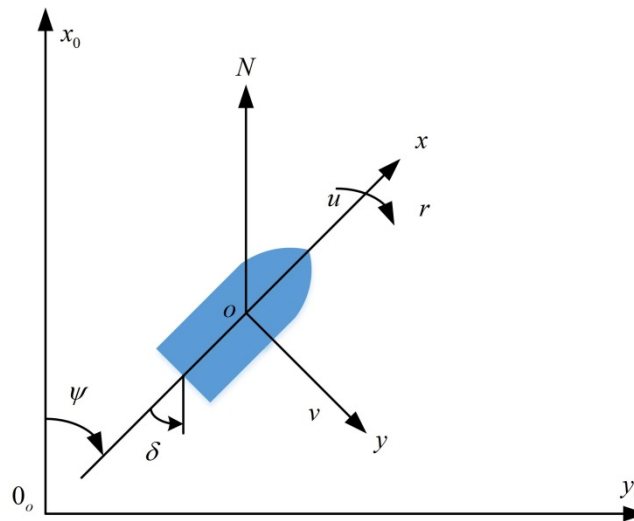


**Figure 3** Ship’s horizontal-plane coordinate system.

For the plane maneuvering motion of surface ships, of most concern is the variation law of heading angle and yaw rate with time  $t$ . In reference to Velagic et al. (2003), when the origin is taken in the ship, the basic equation of ship plane motion in the appendage coordinate system is:

$$\begin{cases} \text{surge: } m(\dot{u} - vr - x_c r^2) = X \\ \text{sway: } m(\dot{v} + ur + x_c \dot{r}) = Y \\ \text{yaw: } I_{ZZ} \dot{r} + mx_c(\dot{v} + ur) = N \end{cases} \tag{4}$$

where  $m$  is the mass of the ship,  $u$  and  $v$  are surge and sway velocities, respectively,  $r$  is the yaw rate,  $I_{ZZ}$  is the moment of inertia about the  $z$ -axis,  $X$  and  $Y$  are forces in the  $x$ -axis direction and the  $y$ -axis direction, respectively,  $N$  is a moment around the  $z$ -axis, and  $r_c = [x_c, y_c, z_c]$  is the center of gravity.

Dyda et al. (2019) simplified the third-order ship model to second-order and obtained the Nomoto model, denoted as transfer function  $G_{r\delta}(s)$ :

$$G_{r\delta}(s) = \frac{r(s)}{\delta(s)} = \frac{K}{Ts + 1} \quad (5)$$

where  $\delta(s)$  is the input (actual rudder angle), and  $r(s)$  is the output (yaw rate). According to  $r = \dot{\psi}$ ,

$$G_{\psi\delta}(s) = \frac{\psi(s)}{\delta(s)} = \frac{K}{s(Ts + 1)} \quad (6)$$

and

$$T\ddot{\psi} + \dot{\psi} = K\delta \quad (7)$$

This is the first-order KT equation of ship maneuvering motion, also known as the Nomoto model. One of the main advantages of the Nomoto model is that the order of the controller is low, and easy to implement (Zhang et al. 2008). Nomoto transfer function (6) is validated for constant course and ship speed; it has also achieved very considerable results in the research of many scholars. However, there is a more practical and accurate method to obtain the transfer function by MATLAB function LINMOD.

The corresponding closed-loop system, shown in **Figure 4**, has the transfer function,

$$\frac{C(s)}{R(s)} = \frac{G_{\psi\delta}(s)}{1 + G_{\psi\delta}(s)H(s)} \quad (8)$$

where  $C(s)$  is the output (course angle) and  $R(s)$  the input (rudder angle),  $G_{r\delta}(s)$  is the open-loop transfer function given by (6), and  $H(s)$  the feedback transfer function which is taken as  $H(s) = 1$  in the present Simulink code (Budak & Beji, 2020). Applying the Routh-Hurwitz stability criterium to the system reveals that the system is stable and, hence, controllable.

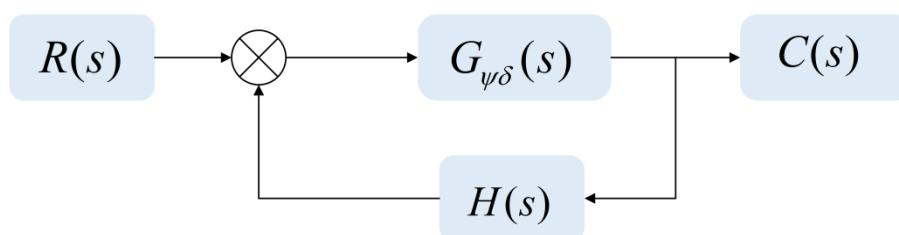


**Figure 4** Block diagram for the closed-loop system for a ship.

The following formula (9) can be obtained by combining Formula 6 and Formula 8 with  $H(s) = 1$ ,

$$G_{\psi\delta}(s) = \frac{K}{s(1 + Ts) + \varepsilon} \quad (9)$$

where  $\varepsilon = K * H(s)$ . Formula 6 itself contains an integrator that can eliminate static errors caused by output interference. However, for the input interference, there is an impact on the static error. The use of MATLAB function LINMOD is equivalent to adding an integral term in Formula 6 and

a very small constant in the denominator; the modified Nomoto model can be expressed as Formula 9.

$K$  is the cyclicity index of the Nomoto model. A larger  $K$  indicates a greater yawing angular velocity and a better turning ability.  $T$  is the following index. A smaller  $T$  indicates a shorter time for a ship to stabilize to a new course and a better steering effect. The relationship between  $T$  and  $K$  is calculated by the following formula (Witkowska & Smierzchalski, 2009):

$$\begin{cases} K = K' v_L / L \\ T = T' L / v_L \end{cases} \quad (10)$$

where  $T'$  and  $K'$  are dimensionless coefficients of the model,  $v_L$  is ship speed, and  $L$  is ship length. The Nomoto model is widely used to analyze the dynamic behavior of ship motion in the field of classical control theory and intelligent control and can be used as the basis for the design of course controllers and path following controllers.

When designing the transfer function of a lead compensator, the Nomoto model, as one of the transfer functions of the original system, is easy to draw, with its corresponding logarithmic amplitude-frequency characteristic  $L_0(w)$ , cut-off frequency  $w_c$ , and phase margin  $\gamma$ . In the field of control (Gao et al., 2007; Borrie, 1987), cut-off frequency  $w_c$  represents the frequency of a point with an amplitude of 0dB on a logarithmic amplitude-frequency characteristic curve. Corresponding logarithmic amplitude-frequency characteristic  $L_0(w)$  represents the relationship between logarithmic amplitude  $20 \lg A(w)$  and cut-off frequency  $w_c$ . Phase margin  $\gamma$  denotes the additional phase angle lag at the cut-off frequency  $w_c$  when the system reaches critical stability.

Thus, considering the first-order Nomoto model of ship dynamics incorporating the steering gear servo model, the following scheme is obtained:

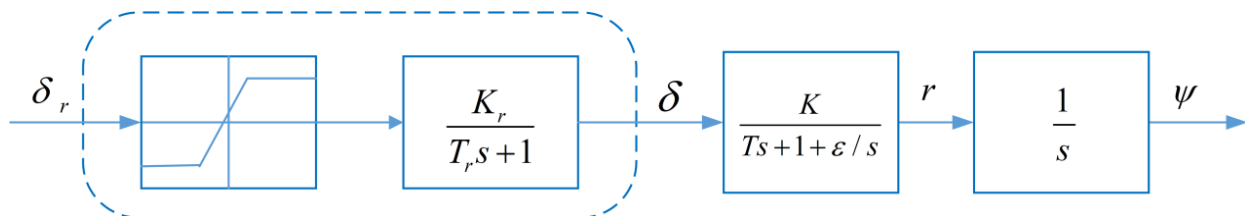


**Figure 5** Linear ship dynamics model, including steering gear servo system.

### 2.3 Environmental disturbances model

When a ship sails in an inland waterway, it is disturbed by the wind, the current, and other external environments, which will cause the ship to swing and deviate from the planned course. Therefore, the random interferences of various disturbances should be taken into account when designing a navigation controller. Reasonable mathematical models should be established for these disturbances.

For wind interference, the average wind can be converted into the wind equivalent rudder angle by using Eq. (11) (Boxu & Zhang, 2021).

$$\delta_w = K \left( \frac{v_w}{v_L} \right) \sin \theta \quad (11)$$

where  $v_w$  is wind speed,  $v_L$  is ship speed,  $K$  is the cyclicity index,  $\theta$  is the yaw angle, and  $\delta_w$  is the wind equivalent rudder angle.

Flow interference is expressed by the change of ship speed. Due to the complexity of the flow characteristics, most ship maneuvering motion modeling is simplified by the assumption of a steady and uniform flow. In the established coordinate system, the flow direction is  $\psi_c$  and the flow rate is  $V_c$ ; then, the components  $u_c$  and  $v_c$  of the flow velocity in the X and Y directions are:

$$\begin{cases} u_c = V_c \cos(\psi_c - \psi) \\ v_c = V_c \sin(\psi_c - \psi) \end{cases} \quad (12)$$

### 3. Adaptive feedforward PID controller design

#### 3.1 PID course autopilot

PID control is one of the earliest developed control strategies. It has a simple algorithm, good robustness, and high reliability (Yang et al., 2011). It is widely used in process control and motion control, especially for deterministic control systems which can establish accurate mathematical models.

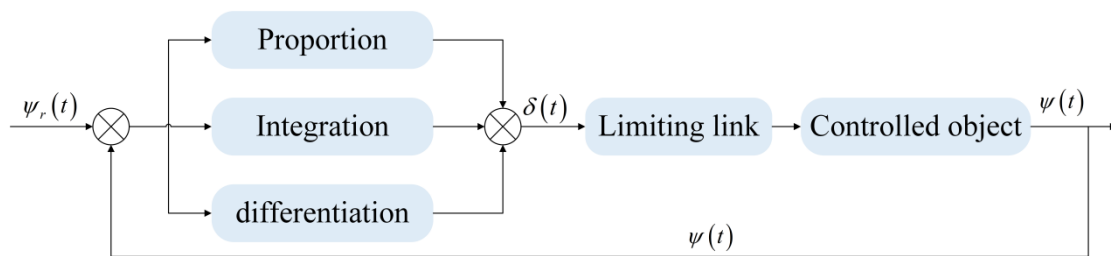


**Figure 6** Principle block diagram of PID course autopilot.

The principle diagram of the PID course autopilot is shown in **Figure 5**. Autopilot forms the course deviation  $\Delta\psi(t) = \psi_r(t) - \psi(t)$  according to course of advance  $\psi_r(t)$  and actual course  $\psi(t)$ . The proportional (P), integral (I), and differential (D) of the course deviation  $\Delta\psi(t)$  are linearly combined to output the rudder angle  $\delta(t)$ , and the rudder angle is controlled between  $[-35^\circ, 35^\circ]$  through the limiting link to control the ship's course, which is called a PID course autopilot. Its control law is:

$$\delta(t) = K_p \left[ \Delta\psi(t) + \frac{1}{T_i} \int_0^t \Delta\psi(t) dt + \frac{T_d d\Delta\psi(t)}{dt} \right] \quad (13)$$

where  $K_p$ : proportionality factor;  $T_i$ : integration time constant; and  $T_d$ : differential time constant. In practical application, even if the instantaneous change of angle can be ignored, it will lead to infinite signal output. So, the ideal derivative term needs to add a filter in practice.

### 3.2 Lead compensator design

#### 3.2.1 Design principle of lead compensator

A compensator with a phase advance characteristic (positive phase shift) is called a lead compensator (Monje et al., 2004). According to the two characteristics of amplitude elevation and phase advance of lead compensator, it is generally set in the middle-frequency of the system. The band near the cut-off frequency is called the middle-frequency band. Because the middle-frequency band has great influence on the dynamic performance of the system, it reflects the stability and

rapidity of the dynamic response of the system (Kumar & Elangovan, 2017). The essence of the lead compensator is to increase the cut-off frequency of the system and improve the rapidity by using the characteristics of high-frequency amplitude elevation of the lead device. It can provide a positive phase shift for the system so that the system phase margin increases and the relative stability is improved (Jiang et al., 2006; Wang et al., 2009). The design of the lead compensator is the process of correctly selecting the 2 parameters  $\alpha$  and  $T$  of the compensator (Nie et al., 2011).  $\alpha$  is the division coefficient of the lead compensator network, and  $T$  is the time constant.

The steering gear servo system is generally driven by a servo mechanism and is itself a feedback control system with nonlinear characteristics such as pure lag and saturation. Moreover, if the steering gear servo system is a hydraulic servo, sometimes two sets of the hydraulic drive are needed to increase the speed of the steering gear and the flexibility of the control. For the majority of ships, the rudder angle and speed of its change are kept within certain limits (Amerongen, 1984). When the crew manipulates it, the ship does not turn immediately after receiving the command rudder angle  $\delta_r$ , requiring a conversion process. So, there is a problem with response time. The essence of a lead compensator is to use a lead device to increase the system cut-off frequency and improve the rapidity. If the response time is accelerated, the angular velocity will also be accelerated. Changing the course will be completed in a short time, saving energy consumption and reducing the occurrence of accidents.

When designing a lead device that meets dynamic performance, the transfer function of the original system should be clarified. The higher the order of the transfer function is, the more difficult it is to compensate for the transfer function (Rohitha et al., 2005). Since the order of the Nomoto model is lower than that of the second-order linear KT equation, the Nomoto model is selected as one of the transfer functions of the original system. **Figure 4** captures the main context of ship dynamics of  $\delta_r \rightarrow \delta \rightarrow r \rightarrow \psi$ , that the steering machine is also a part of a linear ship dynamics model. Therefore, the steering gear servo system is also regarded as one of the transfer functions of the original system.

In the ship feedforward PID controller system, the first input is the course of advance, and the actual ship course is measured by the compass; then, the course deviation value is taken as the input of the ship course keeping controller, to control the output of rudder angle  $\delta$ .

The mathematical model  $W(s)$  of the steering gear servo system and Nomoto model  $G_{\psi\delta}(s)$  are taken as the transfer function  $G_0(s) = W(s) \times G_{\psi\delta}(s)$  of the original system, the corresponding logarithmic amplitude-frequency characteristic  $L_0(w)$  is drawn, and the cut-off frequency  $w_c$  is obtained. According to the calibration principle, the compensator is designed. Firstly, the transfer function  $G_C(s) = (\alpha Ts + 1) / (Ts + 1)$  of the compensator is assumed. Secondly, the corresponding parameters  $\alpha$  and  $T$  are determined, according to the cut-off frequency  $w_c$ . Thirdly, the transfer function  $G(s) = G_0(s) \times G_C(s)$  of the system after correction is determined. Finally, the command rudder angle  $\delta_r$  to be transferred to the transfer function  $G(s)$  of the system after correction is determined to realize the change of ship course. The system structure of the ship feedforward PID controller is shown in **Figure 7**.

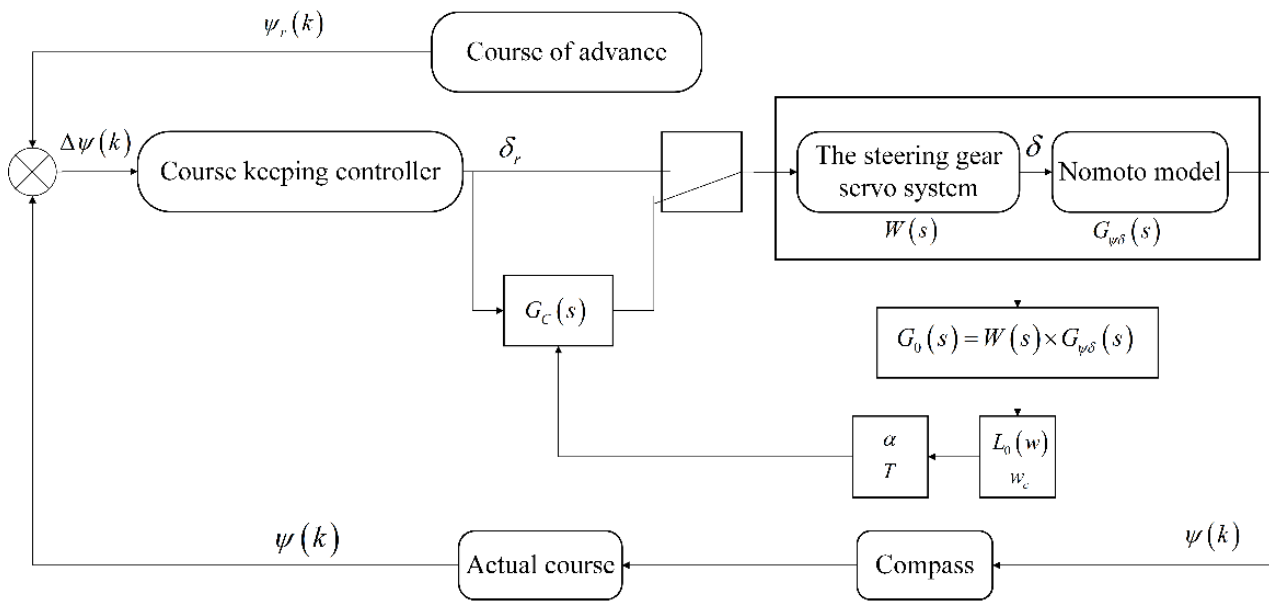


**Figure 7** System structure of ship feedforward PID controller.

### 3.2.2 Design steps of lead compensator

(1) Determine the transfer function  $G_0(s)$  of the original system, draw its corresponding logarithmic amplitude-frequency characteristic  $L_0(w)$ , and calculate the cut-off frequency  $w_c$ . The original transfer function  $G_0(s)$  of the path following control system is determined:

$$G_0(s) = W(s) \times G_{\psi\delta}(s) = \frac{K_r}{T_r s + 1} \times \frac{K}{s(Ts + 1) + \varepsilon} \quad (14)$$

According to the ship parameter table and calculation formula in **Table 2** and Formula 10, draw the corresponding logarithmic amplitude-frequency characteristic curve.

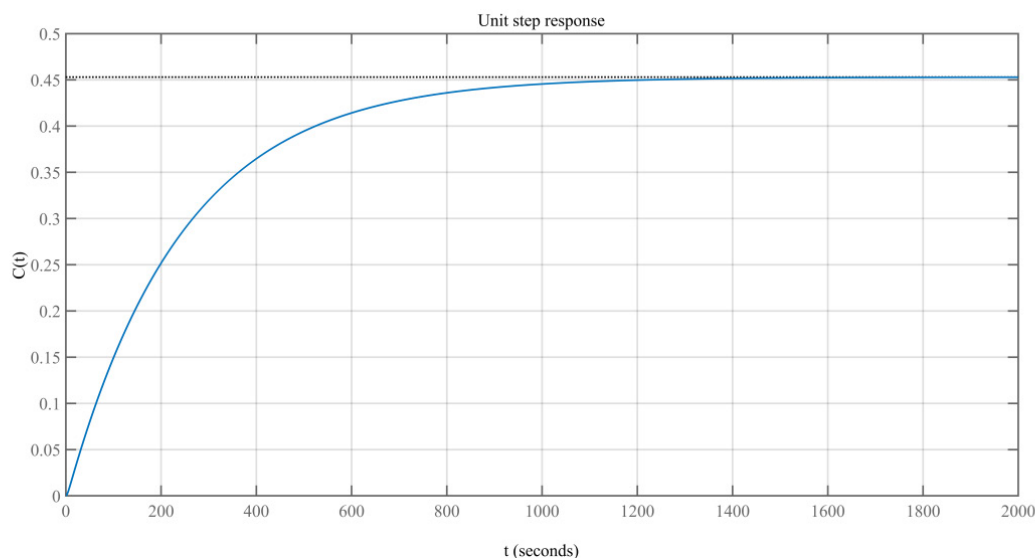


**Figure 8** Time-domain waveforms of the system before compensation.

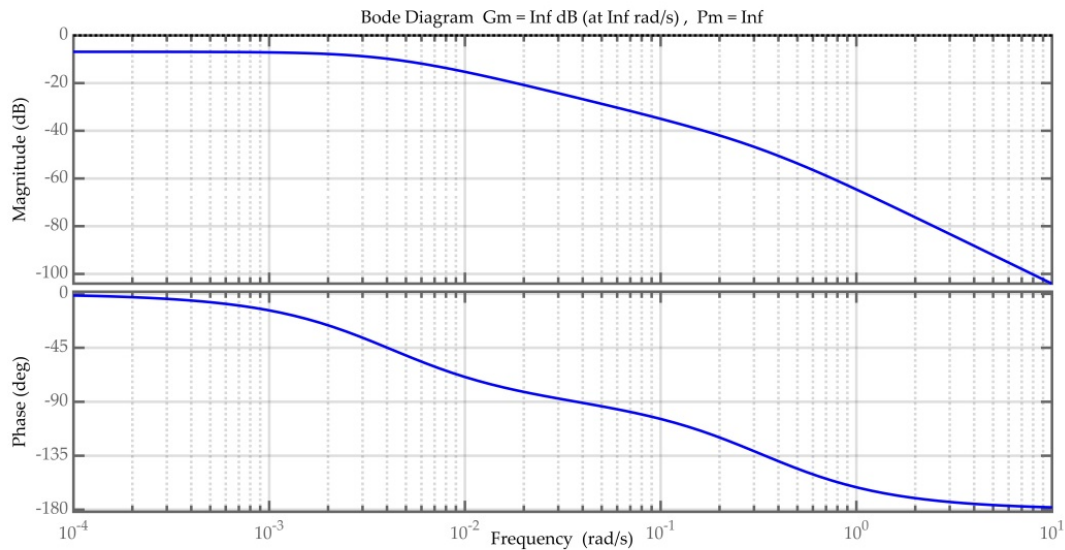


**Figure 9** Bode diagram of the system before compensation.

Where  $C(t)$ : the unit step response curve of the system before compensation. Bode diagram includes a logarithmic amplitude characteristic diagram and a logarithmic phase-frequency characteristic diagram. In the logarithmic amplitude characteristic diagram, the abscissa represents frequency, and the ordinate represents 20 times the logarithm of amplitude  $A(\omega)$ . In the logarithmic phase amplitude characteristic diagram, the abscissa represents frequency, and the ordinate represents the phase angle of frequency characteristic.

It can see from **Figures 8** and **9** that the unit step response of the original system is slow, and the cut-off frequency  $\omega_c$  is about 0.00379.

To accelerate the response of the system and improve the course angular velocity, it is necessary to increase the cut-off frequency of the system. Double the cut-off frequency,  $\omega_m = \omega_{c1} \approx 2\omega_c = 0.007$ .

(2) Design compensator

Set the transfer function  $G_C(s) = (\alpha Ts + 1) / (Ts + 1)$  of the compensator and determine the parameters  $\alpha$  and  $T$ .

According to the compensator principle,  $\omega_m = \omega_{c1} = 0.007$ . To make the amplitude of the post-compensation system be 0 at the cut-off frequency  $\omega_{c1} = 0.007$ , the amplitude of the original system of the compensation should be increased by  $10 \lg \alpha$  at  $\omega_{c1}$ .

$$L_0(\omega_{c1}) \approx -40 \lg \frac{\omega_{c1}}{\omega_c} = -10 \lg \alpha, \text{ that is:}$$

$$\alpha = \left( \frac{\omega_{c1}}{\omega_c} \right)^4 = \left( \frac{0.007}{0.00379} \right)^4 \approx 11.6368 \tag{15}$$

$$\begin{cases} T = \frac{1}{\omega_m \sqrt{\alpha}} = \frac{1}{0.007 \sqrt{11.6368}} \approx 41.8778 \\ \alpha T = 487.3235 \end{cases} \tag{16}$$

The transfer function of the compensator is as follows:

$$G_C(s) = \frac{487.3235s + 1}{41.8778s + 1} \tag{17}$$

(3) Determine the transfer function of the system after correction:

$$\begin{aligned} G(s) &= G_0(s) \times G_C(s) \\ &= \frac{1}{3s + 1} \times \frac{0.453}{s(242.9s + 1) + 0.453} \times \frac{487.3235s + 1}{41.8778s + 1} \end{aligned} \tag{18}$$

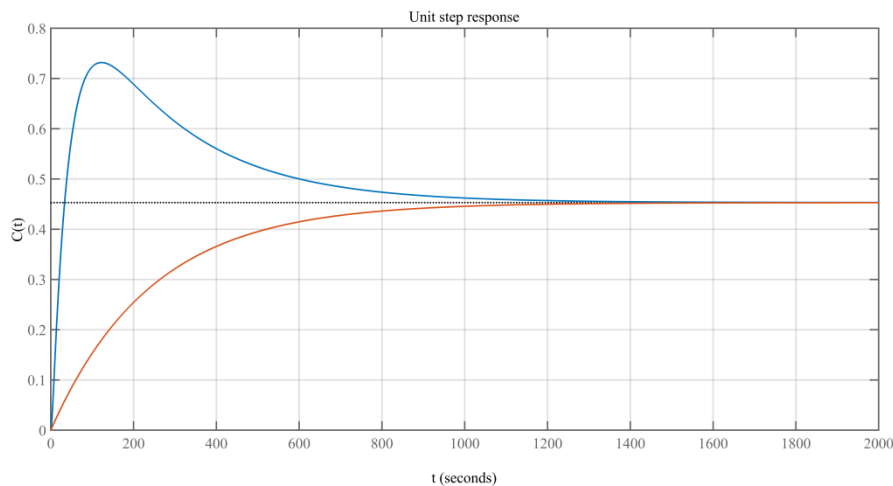


**Figure 10** Time-domain waveforms of the system after compensation.

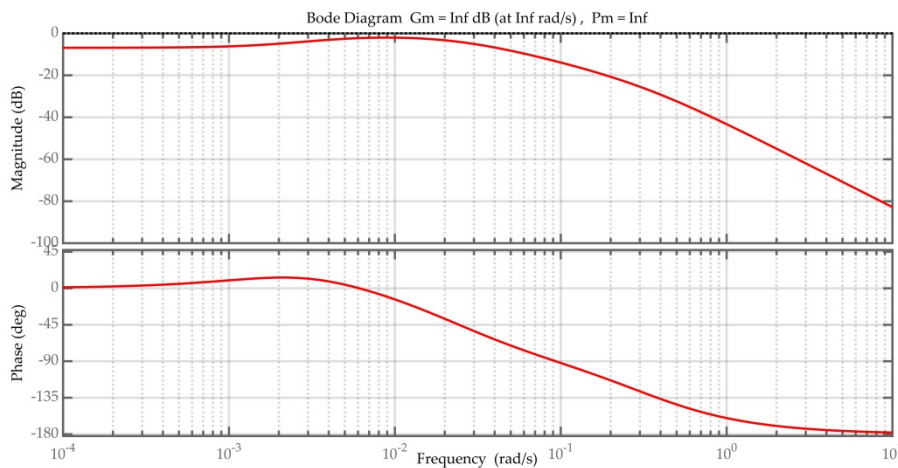


**Figure 11** Bode diagram of the system after compensation.

As can be seen from **Figures 8** and **10**, the unit step response  $C(t)$  of the system after compensation has a smaller overshoot and a shorter adjustment time compared with the unit step response  $C(t)$  of the system before compensation. Therefore, the compensator improves the dynamic performance of the system.

It can be seen from **Figures 9** and **11** that the compensator uses the correction device to change the slope of the intermediate frequency characteristic of the original system; the cut-off

frequency is increased, the phase margin is increased, and the dynamic response speed of the system is improved.

### 3.3 Adaptive feedforward PID controller design

PID control has wide application, a simple structure, and a convenient parameter adjustment. However, the simple PID control law is not perfect for ship course keeping control in dealing with some practical problems. Therefore, the optimal control strategy can be introduced based on PID control.

To improve the accuracy of ship course keeping, in the case of minimum fuel consumption, it is required to reach the target port at the fastest speed, and the whole navigation process is always in the best navigation state. A control scheme, adaptive feedforward PID control is proposed. In this control, the controller is required to automatically adjust the steering gear according to the actual heading, navigation environment, and fuel consumption, so that the whole ship is in the best navigation state at any time, which is helpful for improving the safety and economy of navigation. There are two conditions for ship navigation. One is open sea; at this time, the ship sails at a fixed speed at sea, and the amount of ship steering is less, mainly so as to control fuel consumption. The second is narrow waters; at this time, the amount of ship steering is more, mainly so as to control the accuracy of ship course keeping control. According to different navigation conditions, course keeping and fuel consumption are compromised to make the system operate in the optimal control state.

In a real application, considering ship course keeping and fuel consumption, the quadratic performance index function is selected:

$$J = \int_0^t (e^2 + \lambda \delta^2) dt \tag{19}$$

$e$ : course deviation,

$$e = \psi_r - \psi \tag{20}$$

$\delta$ : rudder angle.

$\lambda$ : weight coefficient.

$J$ : comprehensive evaluation index.

**Table 1** Corresponding table of  $\lambda$  value and wind speeds.

Wind speeds (m/s)	0 - 5	5 - 10	10 - 14	14 - 17	17 - 20	20 - 30	>30
$\lambda$	0.1	4	8	8.5	9	9.5	10

To ensure less fuel consumption, and inhibit ship steering gear,  $\lambda=8\sim 10$ . To improve course accuracy,  $\lambda=0.1$ . The former has a good control effect in rough seas, and the latter has an ideal effect in calm waters (**Table 1**).

The optimal control is to minimize the above quadratic performance index function. According to the theory of linear-quadratic non-zero given point output regulator, the Riccati equation (Saeed, 2012) is:

$$\bar{P}A + A^T \bar{P} - \frac{1}{\lambda} \bar{P}BB^T \bar{P} + C^T C = 0 \tag{21}$$

where  $\bar{P}$ : positive definite symmetric constant matrix.

The state equation and output equation of ship maneuvering are established by using the Nomoto equation:

$$\begin{bmatrix} \dot{\psi} \\ \ddot{\psi} \end{bmatrix} = A \begin{bmatrix} \psi \\ \dot{\psi} \end{bmatrix} + B\delta \quad (22)$$

$$\psi = C \begin{bmatrix} \psi \\ \dot{\psi} \end{bmatrix} \quad (23)$$

$$A = C \begin{bmatrix} 0 & 1 \\ 0 & -\frac{1}{T} \end{bmatrix}, B = \begin{bmatrix} 0 \\ \frac{K}{T} \end{bmatrix}, C = [1 \quad 0] \quad (24)$$

According to the above formula:

$$\bar{P} = \frac{1}{K} \begin{bmatrix} \sqrt{\lambda} \sqrt{1 + \frac{2KT}{\sqrt{\lambda}}} & T\sqrt{\lambda} \\ T\sqrt{\lambda} & \frac{T}{K} \left( \sqrt{1 + \frac{2KT}{\sqrt{\lambda}}} - 1 \right) \lambda \end{bmatrix} \quad (25)$$

The optimal control law can be obtained:

$$\delta^* = -\frac{\psi}{\sqrt{\lambda}} + \frac{1}{K} \left( 1 - \sqrt{1 + \frac{2KT}{\sqrt{\lambda}}} \right) \dot{\psi} \quad (26)$$

Finally, the optimal PD control law can be obtained:

$$\delta = \frac{1}{\sqrt{\lambda}} e - \frac{1}{K} \left( \sqrt{1 + \frac{2KT}{\sqrt{\lambda}}} - 1 \right) \dot{e} \quad (27)$$

That is,

$$K_p = \frac{1}{\sqrt{\lambda}}, K_d = \frac{1}{K} \left( \sqrt{1 + \frac{2KT}{\sqrt{\lambda}}} - 1 \right) \quad (28)$$

$K, T$  are solved as Formula (10). According to the formulas in **Table 2**,  $K > 0, T > 0, \lambda > 0$ , so the closed-loop control system is asymptotically stable.

**Table 2** Ship parameter list and calculation formula of  $K'$ ,  $T'$ .

Parameters	Symbol	Value	Units
Ship length	$L$	126	$m$
Ship draught	$D$	5	$m$
Ship width	$B$	20.8	$m$
Rudder area	$A_R$	18.8	$m^2$
Block coefficient	$C_b$	0.681	
Aspect ratio of the rudder	$\lambda$	1.72	
Disk ratio	$\theta$	0.67	
Number of blades	$Z$	4	
Propeller pitch	$P$	3.66	$m$
Propeller	$D_P$	4.6	$m$

$$K' = 47.875 - 2.64L / B + 0.004Ld / A_R + 66.589Cb^2 - 112.702Cb + 3.826Cb \times L / B - 0.293Cb \times B / d$$

$$T' = 26.464 + 0.408Cb \times L \times d / A_R - 0.033L^2 \times d / (A_R \times B) - 79.114Cb + 0.757L / B + 46.129Cb^2$$

Weight coefficient:

$$\lambda = \frac{1}{2} \left( \sqrt{2 + \frac{\sqrt{\lambda}}{KT}} \right) \quad (29)$$

Natural frequency:

$$w_n = \sqrt{\frac{K}{T\sqrt{\lambda}}} \quad (30)$$

$K_i$  can be obtained by introducing  $w_n$  into the solution formula of  $K_i$ , the parameter of conventional PID controller:

$$K_i = \frac{1}{10} \left( \sqrt{\frac{K}{T\sqrt{\lambda^3}}} \right) \quad (31)$$

### 3.4 Path following in inland waterways

Intended path is composed of the straight-line segment and the positive arc turning segment, which are called the direct navigation process and the turning navigation process, respectively. Navigation deviation includes path following deviation and course deviation, in which path following deviation refers to the shortest distance from the current ship to the current segment, and course deviation refers to the deviation between the current ship's course and the course of advance. In this paper, the equal course method is used to calculate the course deviation and the path following deviation.

### 3.4.1 Navigation control of straight-line segment

Most of the time, the ship sails in the straight-line segment. The ship plans to navigate from point A to point B, and a bearing of destination B relative to the starting point A is the intended course  $\psi_o$ . Due to the influence of wind, flow, and other factors in navigation, the ship yaws to point P at a certain time, and ship course at point P is  $\psi_n$ .

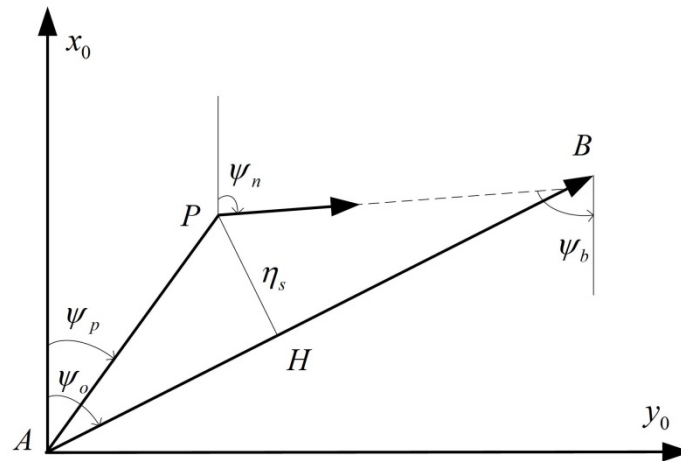


**Figure 12** Navigation control of straight-line section.

Course deviation:

$$\Delta\psi_s = \psi_n - \psi_o \tag{32}$$

The bearing angle of point P relative to the starting point A is  $\psi_p$ . The bearing angle of point P relative to the ending point B is  $\psi_b$ , and its difference from intended course is  $\beta$ ,

$$\beta = \psi_b - \psi_o \tag{33}$$

The intersection of point P and segment AB is H, the distance from point P to segment AB is PH, the distance from point P to point B is PB, and PH is path following deviation.

$$\eta_s = PB \sin \beta \tag{34}$$

### 3.4.2 Navigation control of turning segment

The whole route is composed of segments connected by multiple waypoints. When the ship sails on these segments, altering course between segments is formed. When the ship turns from one segment to the next, it is realized through a turning transition arc. When the ship is sailing in a transition arc, calculations of course deviation and path following deviation need to be considered separately. To allow the ship to quickly follow the new course after turning, it is necessary to increase the path following control accuracy of the turning segment.

As shown in **Figure 13**, the straight-line segment AD and the straight-line segment DF form a steering segment. According to current speed and turning radius, an arc is planned to make it tangent to two straight-line segments at the same time. Through the following control, the ship smoothly transits from AD to DF along the arc. Due to the inertia, the ship does not steer immediately after receiving the steering command. It produces a retention distance BC, and then the ship begins to turn steadily.

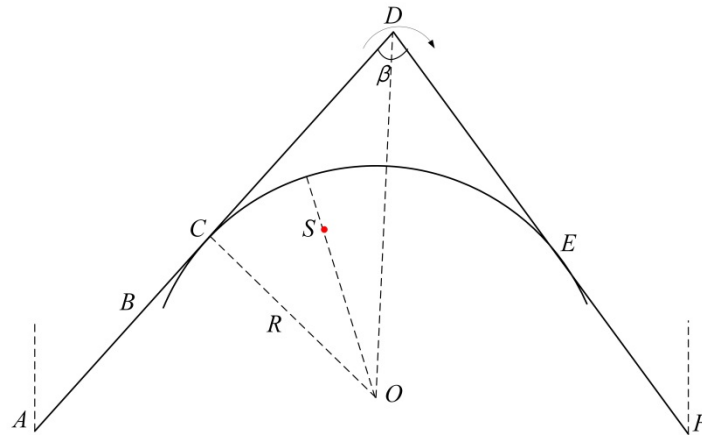


**Figure 13** Navigation control of turning segment.

In **Figure 13**,  $A(x_A, y_A)$ ,  $D(x_D, y_D)$ ,  $F(x_F, y_F)$  is the waypoint of the intended path,  $S(x_S, y_S)$  is the position of the ship, and  $R$  is the arc radius of the turning segment. Determining the path following deviation and course deviation:

1) Determine the direction of the turning transition curve:

$$F = \text{sign}[\sin(\theta_{DF} - \theta_{AD})] \quad (35)$$

2) Determine the center coordinates of the turning transition curve  $O(x_O, y_O)$

The angle between segment AD and segment DF:

$$\beta = \pi - F \times (\theta_{DF} - \theta_{AD}) \quad (36)$$

$D_{OD}$  is the distance from D to the turning center O:

$$D_{OD} = R / \sin(\beta / 2) \quad (37)$$

$\theta_{OD}$  is the angle between the vector direction of the turning center O to D and the due north direction:

$$\theta_{OD} = \theta_{AD} - F \times (\beta / 2) \quad (38)$$

Determine the coordinates of the point  $O(x_O, y_O)$ :

$$\begin{pmatrix} x_O \\ y_O \end{pmatrix} = \begin{pmatrix} x_D \\ y_D \end{pmatrix} - D_{OD} \begin{pmatrix} \sin \theta_{OD} \\ \cos \theta_{OD} \end{pmatrix} \quad (39)$$

3) Calculation of course deviation and path following deviation (supposing the course of the ship is  $\psi_s$ )

Path following deviation:

$$\eta_t = (\sqrt{(x_O - x_S)^2 + (y_O - y_S)^2} - R) \times F \quad (40)$$

Course deviation:

$$\Delta\psi_t = \psi_s - \arctan[(y_O - y_S)/(x_O - x_S)] \quad (41)$$

#### 4) Precision control of turning segment

The ship starts to steer  $\delta_0$  at point B. Due to the inertia, the ship is still sailing along the original straight-line at the original speed  $v$  at the beginning. BC calls the retention distance:

$$BC = v(T + t_1 / 2) \quad (42)$$

where  $T$ : the following index of Nomoto model.

$t_1$ : the time of rudder angle from 0 to  $\delta_0$ . Assuming that  $0 - 35^\circ$  takes 15 s, then  $t_1 = \frac{15}{35} \delta_0$ .

Assuming that the ship cycles immediately after the retention distance:

$$\begin{cases} r_0 = K\delta_0 \\ Rr_0 = v' \\ CD = R / \tan(\beta / 2) \end{cases} \quad (43)$$

$r_0$ : Rotational angular rate at steady rudder angle  $\delta_0$ ,

$R$ : radius of gyration,

$K$ : cyclicity index of Nomoto model.

$$CD = \frac{180v'}{\pi K \delta_0} / \tan(\beta / 2) \quad (44)$$

$$BD = v(T + t_1 / 2) + \frac{180v'}{\pi K \delta_0} / \tan(\beta / 2) \quad (45)$$

### 3.5 Indirect path following control system

The principle of the indirect path following control system is shown in **Figure 14**. The indirect control scheme divides the control into three nested loops. The function of the outer loop (path loop) is to compare the ship position data received by GPS with the intended route to obtain the path following deviation information  $\eta(k)$ . A command course  $\psi_r(k)$  to the course keeping loop is obtained by the path keeping algorithm, which guides the ship to move in the direction of eliminating path following deviation. The middle loop (course keeping loop) compares  $\psi_r(k)$  with the actual course  $\psi(k)$ , collected by compass, to form course deviation information  $\Delta\psi(k) = \psi_r(k) - \psi(k)$ . A command rudder angle  $\delta_r(k)$  to the rudder angle control loop is obtained by course keeping algorithm, which makes the ship navigate in the direction of reducing course deviation. The inner loop (rudder angle control loop) is used to drive the rudder so that the rudder angle detection value  $\delta(k)$  is consistent with the rudder angle command; finally, the path is maintained.

In terms of control effect, there is  $\delta(k) \Rightarrow \Delta\psi(k) \rightarrow 0 \Rightarrow \eta(k) \rightarrow 0$ , which controls the course deviation  $\Delta\delta(k)$  and path following deviation  $\eta(k)$  sequentially from the rudder angle. The indirect path following control scheme can obtain better control accuracy, which is suitable for

high-precision control occasions. It is necessary to control the ship in a limited channel, which can ensure safety in the complex segment of inland waterways and bridge areas, so the scheme is selected.

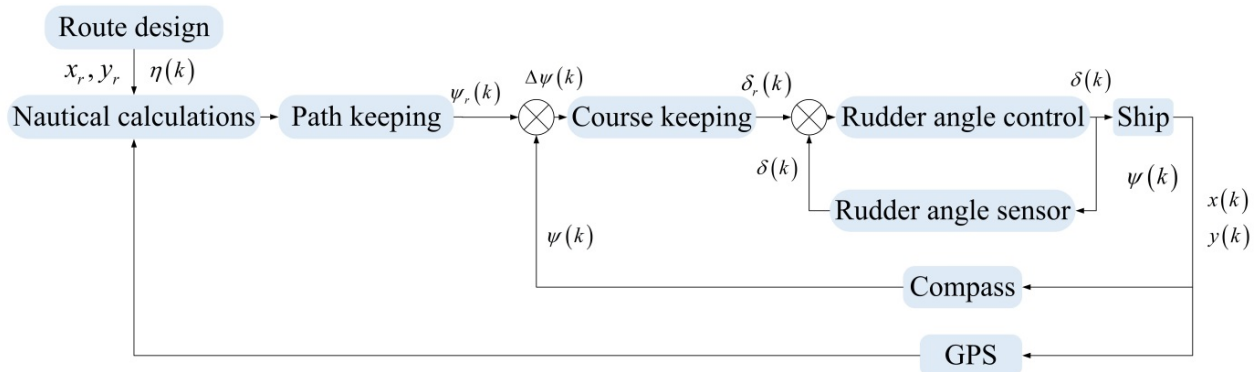


Figure 14 Principle block diagram of indirect path following control system.

Path following is the trajectory of a ship moving over time in a fixed coordinate system. It can be obtained by surging velocity  $u$ , sway velocity  $v$ , and heading angle  $\psi$ :

$$\begin{cases} x = \int_0^t (u \cos \psi - v \sin \psi) dt \\ y = \int_0^t (u \sin \psi + v \cos \psi) dt \end{cases} \quad (46)$$

### 3.6 Determination of rudder angle

Figure 15 shows the block diagram for rudder angle determination with PID control and adaptive feed forward control. Route (1) uses PID to control the rudder angle, and route (2) uses adaptive feedforward PID to control the rudder angle.

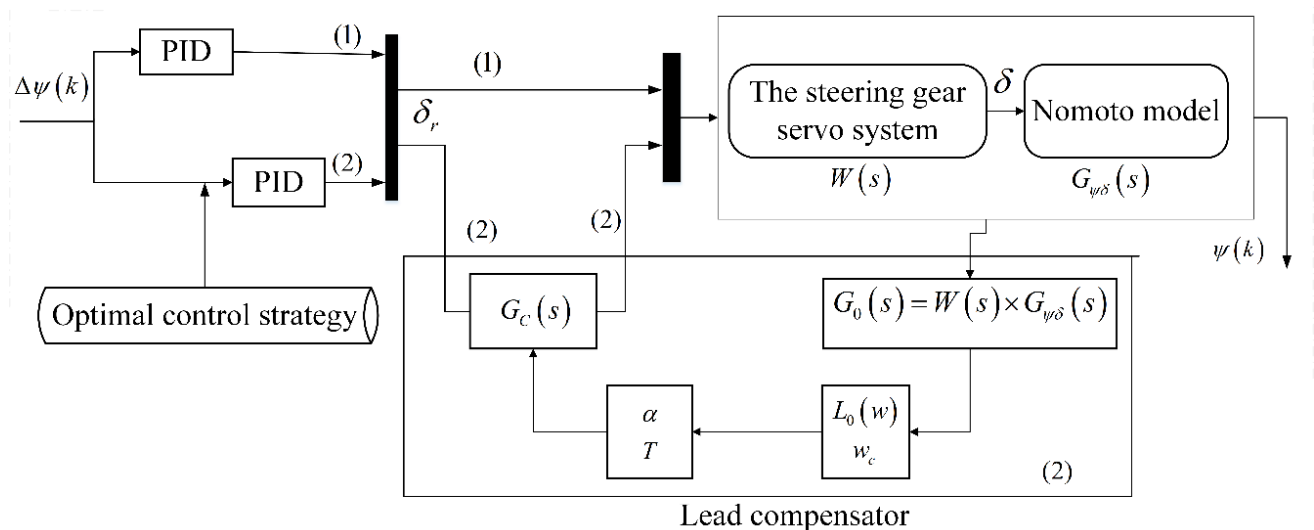
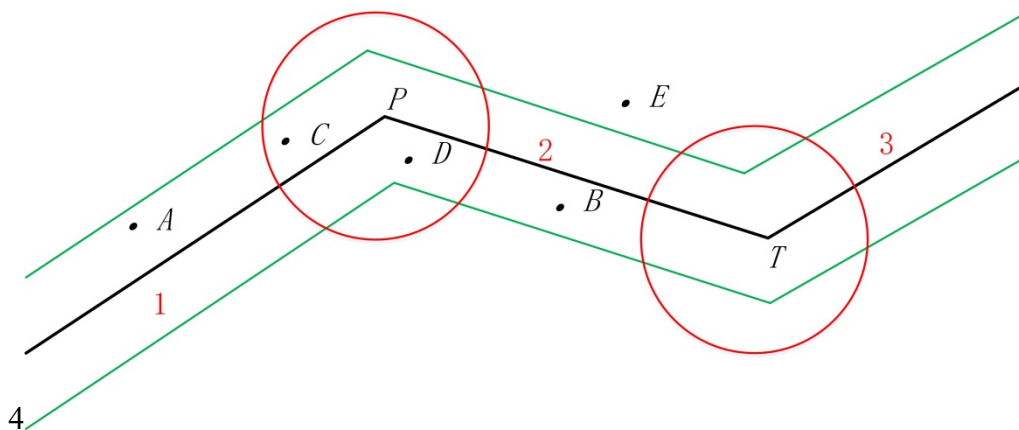


Figure 15 Block diagram for rudder control.

### 3.7 Route segment following

The significance of route segment following lies in whether the next segment can be determined according to the status information, such as the current position and course of the ship. It can reduce unnecessary detours and voyage, reduce the power consumption of control machinery and propulsion machinery, save fuel, and reduce pollution. The input of the system includes the segment number, ship position, and course information. Through the determination of the route segment following algorithm, the segment number to be followed by the ship is removed. The principle of route segment following is shown in **Figure 16**.



**Figure 16** Route segment following.

In **Figure 16**, the black line is the intended route, and P, T is the waypoint of the intended route, the area within the 2 green lines is the specified area of navigation. When the ship turns, its advance steering distance has a great influence on the navigation error and steering when the segment is switched. To ensure the safety of navigation, the circle is drawn with a waypoint as the center of the circle and advance steering distance as the radius R. When the ship sails into the circular area, it will start to alter course between segments. The following lists several position relationships between the ship and the intended segments.

(1) When the ship reaches point A, the distance from the waypoint P is greater than the advance steering distance. According to the algorithm of route segment following, the ship continues to sail along section 1.

(2) When the ship reaches point B, the distance from the waypoint T is greater than the advance steering distance. According to the algorithm of route segment following, the ship continues to sail along section 2.

(3) When the ship reaches point C, the distance from the waypoint P is less than the advance steering distance. According to the algorithm of route segment following, the ship should alter course to section 2 to continue sailing.

(4) When the ship reaches point D, the distance from the waypoint P is less than the advance steering distance. According to the algorithm of route segment following, the ship continues to sail along section 2.

(5) When the ship is sailing at point E, it is outside the specified areas. We establish the line between point E and the nearest waypoint, establish the line between the nearest waypoint and the last waypoint, and calculate the angle B between the 2 lines. If  $\beta \geq 90^\circ$ , the segment is composed of the nearest waypoint, and the previous waypoint is the segment to be navigated.

Figure 17 shows a flow chart of the route segment following algorithm.

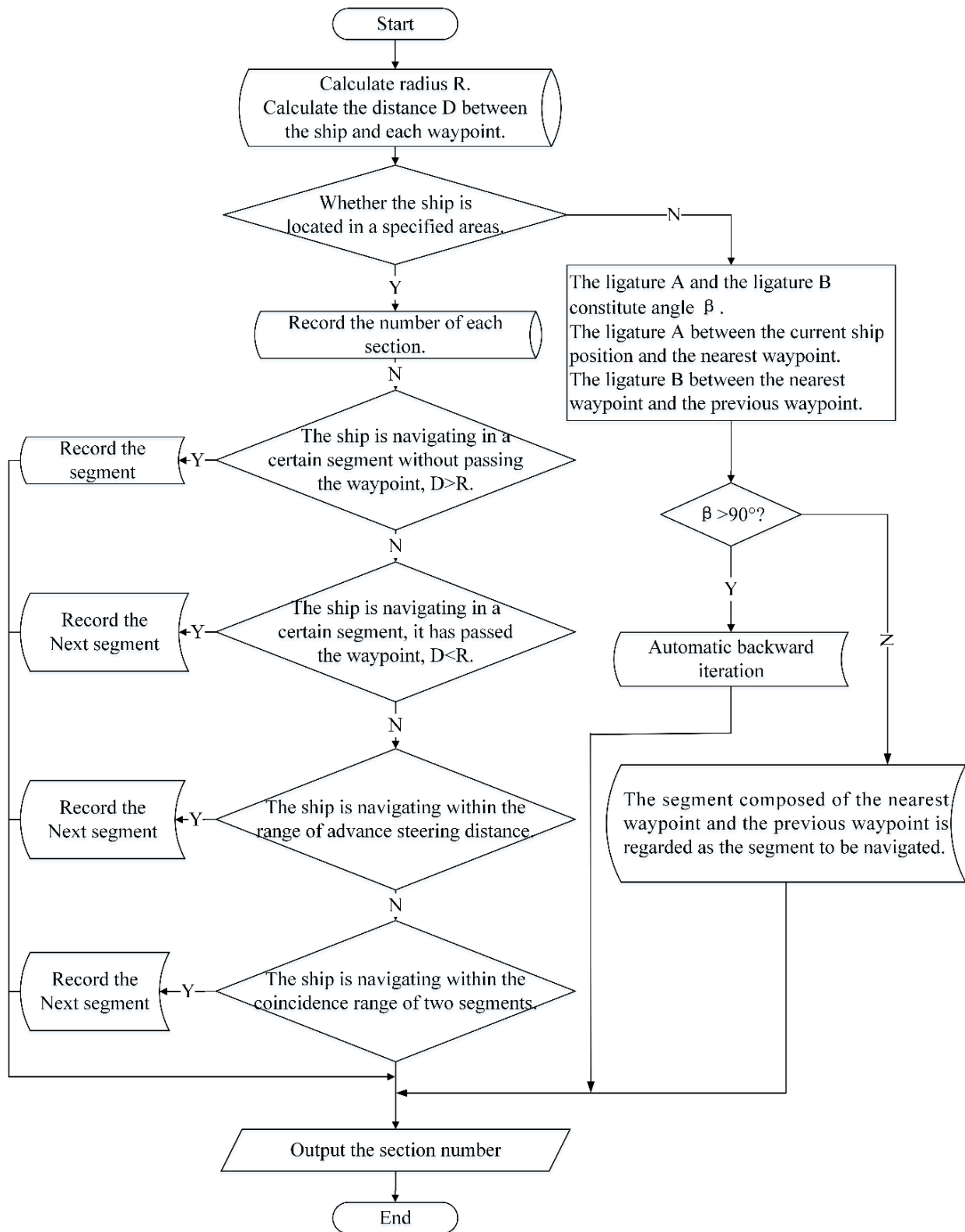


Figure 17 Flow chart of route segment following algorithm.

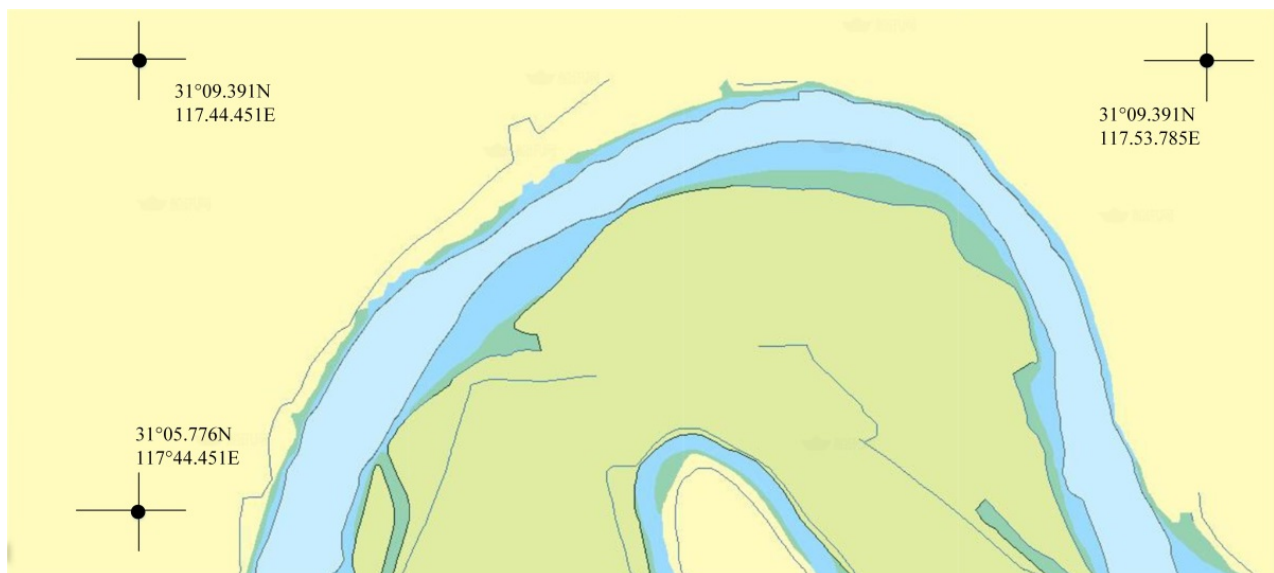
#### 4. Simulation

For verifying the effectiveness and superiority of the proposed control algorithm, this paper uses Simulink to build a simulation platform based on the principle of ship path following control. The parameters of the ship motion model, rudder, and disturbances are designed as adjustable states, and the course, rudder angle, and path following deviation of the ship in the process of motion are output synchronously.

In order to make the control system adapt to different navigation environments, simulation scenarios (divided into environmental disturbance and no disturbance) were designed to verify the performance of the path following control algorithm, using the lead compensator device. In the simulation, the control modes include conventional PID control and adaptive feedforward PID control.

##### 4.1 Path following control experiment in simulation scene

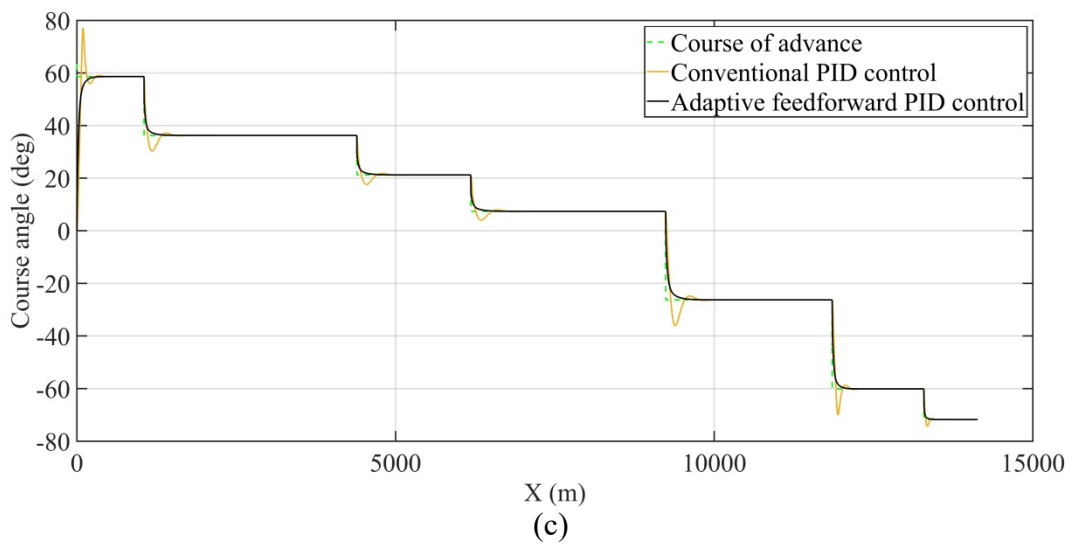
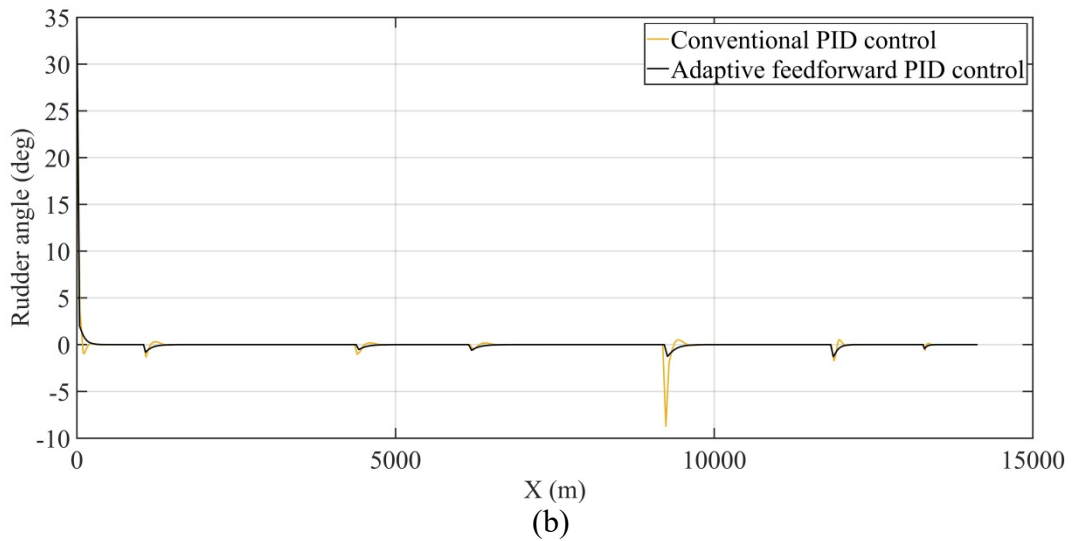
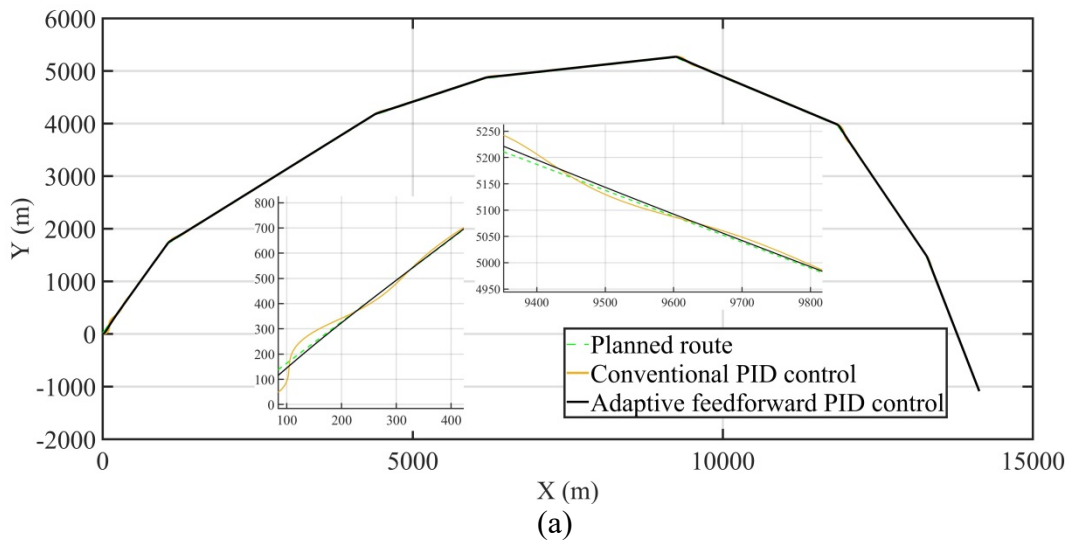
The inland waterway is narrow and tortuous, and the navigation environment is complex. This paper takes **Figure 18** as the studied water area.



**Figure 18** Studied water area.

A multi-section segment composed of multiple waypoints is set up for verifying the effect of the proposed strategy when the advance turning action is considered. The coordinates of the 8 waypoints are (0m, 0m), (1054m, 1730m), (4393m, 4180m), (6157m, 4874m), (9237m, 5270m), (11850m, 3980m), (13290m, 1478m), and (14135m, -1086m). The initial position of the ship is (0m, 0m), and the initial course angle is 63 degrees. The simulation time is 3000s,  $v_L = 5m/s$ ,  $\lambda = 0.1$ . For ship parameters, refer to **Table 2**. Based on this, the parameter of the Nomoto model can be calculated as  $K = 0.453s^{-1}$ ,  $T = 242.900s$ . To make the simulation more consistent with the practice, the characteristics of the steering gear servo system, including the rudder angle saturation limit, steering speed limit, and an integral component, are considered (Boxu & Zhang, 2021). The maximum rudder angle  $\delta_{max}$  is 35 degrees, and the maximum steering speed is 2.7 degrees/s (Thomsen et al., 2014). The control algorithms are conventional PID and adaptive feedforward PID. The path following effect, rudder angle, course, and path following deviation are shown in **Figures 19** and **20**.

(1) Path following control test in calm water environment



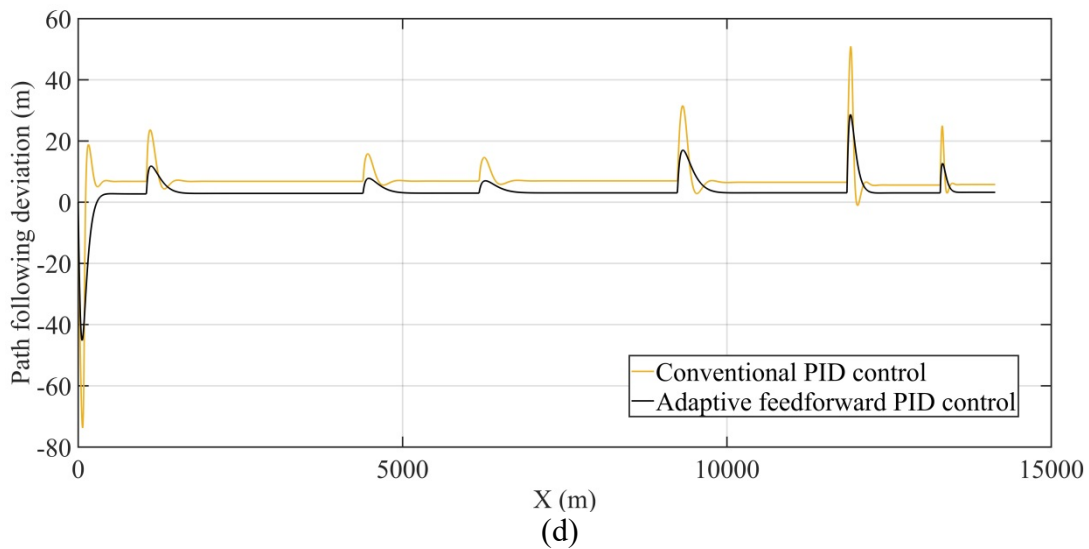
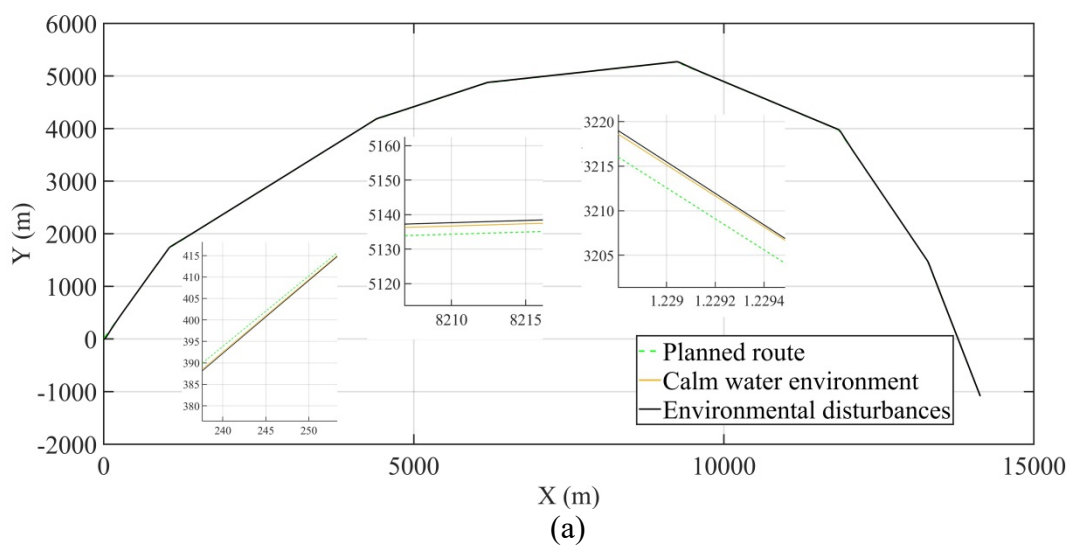


**Figure 19** Simulink results of path following control (calm water environment).

In the path following control test of the simulation scene (calm water environment), the maximum path following deviation is 51 m, and the maximum course deviation is 19 degrees, under conventional PID control. At the same time, the maximum path following deviation is 24 m, and the maximum course deviation is 3 degrees, under adaptive feedforward PID control. In the straight-line segment, the course deviation and path following deviation of the ship tend to 0 with time, and the rudder angle is kept at 0 degrees. In the turning segment, the navigation deviation under adaptive feedforward PID control is lower than that under conventional PID control.

(2) Path following control test in environmental disturbances

For environmental disturbances, of equivalent wind rudder angle  $\delta_w = 2$  degrees, the flow interference is expressed by Eq. (12).



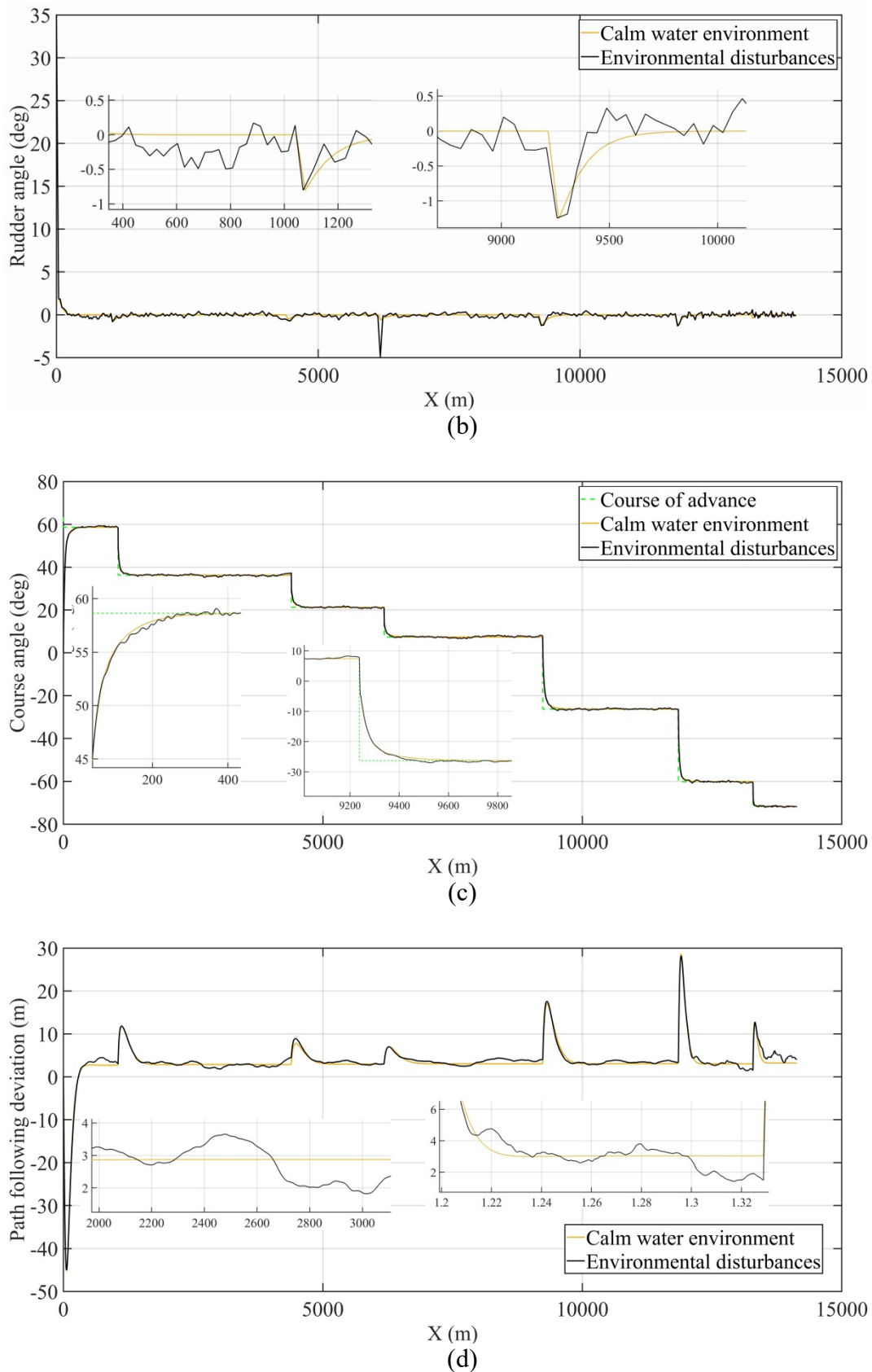


Figure 20 Simulink results of path following control (environmental disturbances).

In the simulation scenario, environmental disturbances are added, which can be seen from the path following control test: when the ship is following each segment, the course deviation of the ship with environmental disturbances will be larger than that in the calm water environment.

The navigation path will swing around the intended path to a certain extent, which is consistent with the actual situation. This is because, under the interference of wind and flow, the path following deviation will deviate slightly from the wind direction compared with the calm water environment.

#### 4.2 Summary

(1) From the above experimental results, the path following deviation and course in the path following control simulation system with a lead compensator are lower than those in the path following simulation system with conventional PID control. It is also suitable for a ship continuing to sail in different types of segments and in environmental disturbances. It shows that the path following control system designed in this paper can effectively complete path following. These control indexes are conformed to the actual situation of ship navigation, and the ship's path keeping performance is improved.

(2) When the ship moves to the area with the waypoint as the center and advance steering distance as the radius, the ship's course is altered. At this time, the mutation of path following error is the error between the current position and the next path section. However, in actual navigation, due to the inertia, the ship will not immediately alter course to follow the next segment, so the path following error of the simulation is larger than the actual path following error. From the rudder angle diagram, it can be seen that the steering times of the system with a lead compensator are very small, which effectively reduces wear in steering gear and reduces the power consumption of control machinery and propulsion machinery.

(3) The path following deviation and course under environmental disturbances will be larger than that of a calm water environment. The deviation amplitude is positively correlated with the interference size, indicating that the designed path following control system also has a certain anti-interference ability.

#### 5. Conclusions

Based on the establishment of the steering gear servo system and the Nomoto model, the design of the lead compensator and adaptive feedforward PID controller, the proposal of the route segment following algorithm, and the analysis of the experimental results, the following conclusions can be drawn.

(1) Under a calm water environment and under environmental disturbances, the ship can navigate along the intended path. It shows that the designed controller has good anti-interference ability.

(2) By comparing the conventional PID path following control scheme with the adaptive feedforward PID path following control scheme, it is proved that the designed adaptive feedforward PID controller is practical and reasonable in the path following control scheme, and its comprehensive performance is better than that of a single controller.

(3) The path following control system can control the ship to navigate along the intended path, which shows that the design of the path following controller and the algorithm of route segment following are reasonable and feasible.

#### References

- Adolphe, K., Zhang, Y., Mbyamm, M., & Ouattara, S. (2020). PID controller parameters enhanced founded on Artificial Fish Swarm Algorithm. *Journal of Physics: Conference Series*, 1457, 012003. doi:10.1088/1742-6596/1457/1/012003
- Amerongen, J. V. (1984). Adaptive steering of ships: A model-reference approach to improved

- manoeuvring and economical course keeping. *Automatica*, 20(1), 3-14. doi: 10.1016/0005-1098(84)90060-8
- Bhattacharya, S., & Gupta, D. (2014). Target path iteration method for trajectory control of ships. *Applied Ocean Research*, 48, 55-65. doi:10.1016/j.apor.2014.07.012
- Børhaug, E., Pavlov, A., & Pettersen, K. Y. (2008). *Integral LOS control for path following of underactuated marine surface vessels in the presence of constant ocean currents* (pp. 4984-4991). In Proceedings of the 47<sup>th</sup> IEEE Conference on Decision and Control 2008. Cancun, Mexico. doi:10.1109/CDC.2008.4739352
- Børhaug, E., Pavlov, A., Panteley, E., & Pettersen, K. Y. (2011). Straight line path following for formations of underactuated marine surface vessels. *IEEE Transactions on Control Systems Technology*, 19(3), 493-506. doi:10.1109/TCST.2010.2050889
- Borrie, J. (1987). Modern control systems: A manual of design methods. *Automatica*, 23(6), 804-805. doi:10.1016/0005-1098(87)90045-8
- Boxu, M., & Zhang, X. (2021). Concise robust fuzzy nonlinear feedback track keeping control for ships using multi-technique improved LOS guidance. *Ocean Engineering*, 224, 108734. doi:10.1016/j.oceaneng.2021.108734
- Breivik, M., & Fossen, T. (2004). Path following for marine surface vessels. *IEEE Techno-Ocean*, 4, 2282-2289. doi:10.1109/OCEANS.2004.1406507
- Budak, G., & Beji, S. (2020). Controlled course-keeping simulations of a ship under external disturbances. *Ocean Engineering*, 218, 108126. doi: 10.1016/j.oceaneng.2020.108126
- Cheng, X., Zhou, C., Zhou, L., Gan, L., Xiao, C., & Jiang, F. (2019). *Research on ship track control in bridge area based on differential evolution algorithm* (pp. 215-221). In Proceedings of the 5<sup>th</sup> International Conference on Transportation Information and Safety 2019. Liverpool, UK. doi:10.1109/ICTIS.2019.8883781
- Cheng, Z., & Hong, X. (2012). *PID controller parameters optimization based on artificial fish swarm algorithm* (pp. 265-268). In Proceedings of the 5<sup>th</sup> International Conference on Intelligent Computation Technology and Automation. Zhangjiajie, China. doi:10.1109/icicta.2012.73
- Chengming, Y., & Zaojian, L. (2018). A fuzzy PID autopilot for ship steering based on membership function optimized by an improved genetic algorithm. *Journal of Multiple-Valued Logic & Soft Computing*, 30(4-6), 559-572.
- Deng, Y., Xianku, Z., & Guoqing, Z. (2019). Fuzzy logic based speed optimization and path following control for sail-assisted ships. *Ocean Engineering*, 171, 300-310. doi:10.1016/j.oceaneng.2018.11.006
- Do, K. D. (2016). Global robust adaptive path-tracking control of underactuated ships under stochastic disturbances. *Ocean Engineering*, 111, 267-278. doi:10.1016/j.oceaneng.2015.10.038
- Do, K. D., & Pan, J. (2004). State- and output-feedback robust path-following controllers for underactuated ships using Serret-Frenet frame. *Ocean Engineering*, 31, 587-613. doi:10.1016/j.oceaneng.2003.08.006
- Do, K. D., Jiang, Z. P., & Pan, J. (2004). Robust adaptive path following of underactuated ships. *Automatica*, 40, 929-944. doi:10.1016/j.automatica.2004.01.021
- Du, J., Xin, H., & Sun, Y. (2017). Adaptive robust nonlinear control design for course tracking of ships subject to external disturbances and input saturation. *IEEE Transactions on Systems, Man, and Cybernetics: Systems*, 50(1), 193-202. doi:10.1109/TSMC.2017.2761805
- Dyda, A. A., Chinchukova, E. P., Oskin, D. A., & Monteriù, A. (2019). *An effective and simple adaptive algorithm for ship course control systems* (pp. 1-6). In Proceedings of the 2019 International Multi-Conference on Industrial Engineering and Modern Technologies. Vladivostok, Russia. doi:10.1109/FarEastCon.2019.8933822
- Format, I. P. (2014). A novel adaptive neural control scheme for uncertain ship course-keeping

- system. *Sensors & Transducers Journal*, 178(9), 282-285.
- Fossen, T. (2011). *Handbook of marine craft hydrodynamics and motion control*. John Wiley & Sons, 2011. doi:10.1002/9781119994138
- Gao, M. Z., Huang, X., & Hong, J. P. (2007). Application of MATLAB and simulink in teaching of automatic control principles. Retrieved from [http://en.cnki.com.cn/Article\\_en/CJFDTotal-HBSF200701025.htm](http://en.cnki.com.cn/Article_en/CJFDTotal-HBSF200701025.htm)
- He, X., Chen, W., Zhu, B., & Cook, C. (2011). Multifactor optimization of a fuzzy-PID controller using genetic algorithm. *Advanced Materials Research*, 422, 268-275. doi:10.4028/www.scientific.net/AMR.422.268
- Jiang, M., Zhang, Z. K., & Dong, D. Y. (2006). A quantum switching architecture on the basis of limited nonlocal operation. *The Journal of China Universities of Posts and Telecommunications*, 13(4), 91-94, doi:10.1016/S1005-8885(07)60041-7
- Kahveci, N., & Ioannou, P. (2013). Adaptive steering control for uncertain ship dynamics and stability analysis. *Automatica*, 49, 685-697. doi:10.1016/j.automatica.2012.11.026
- Kumar, E., & Elangovan, G. (2017). Cascade PID-lead compensator controller for non-overshoot time responses of unstable system. *Energy Procedia*, 117, 708-715. doi:10.1016/j.egypro.2017.05.185
- Li, Z., Hu, J., & Huo, X. (2012). *PID control based on RBF neural network for ship steering* (pp. 1076-1080). In Proceedings of the 2012 World Congress on Information and Communication Technologies. Trivandrum, India. doi:10.1109/WICT.2012.6409235
- Liangqi, L., Renxiang, B., Wuchen, S., & Xinyu, L. (2019). *Ship track-keeping control based on sliding mode variable structure pid controller and particle swarm optimization* (pp. 887-891). In Proceedings of the 6<sup>th</sup> International Conference on Information Science and Control Engineering. Shanghai, China. doi:10.1109/ICISCE48695.2019.00180
- Liu, L., Wang, D., & Peng, Z. (2015). Path following of marine surface vehicles with dynamical uncertainty and time-varying ocean disturbances. *Neurocomputing*, 173, 033. doi:10.1016/j.neucom.2015.08.033
- Monje, C., Calderón, A., Vinagre, B., & Feliu, V. (2004). *The fractional order lead compensator* (pp. 347-352). In Proceedings of the 2<sup>nd</sup> IEEE International Conference on Computational Cybernetics. Vienna, Austria. doi :10.1109/ICCCYB.2004.1437746
- Moreira, L., Fossen, T., & Guedes, C. S. (2007). Path following control system for a tanker ship model. *Ocean Engineering*, 34, 2074-2085. doi:10.1016/j.oceaneng.2007.02.005
- Nie, Z. Y., Wang, Q. G., Wu, M., & He, Y. (2011). Lead/Lag compensator design for unstable delay processes based on new gain and phase margin specifications. *Industrial & Engineering Chemistry Research*, 50(3), 133001337. doi: 10.1021/ie1007322
- Perera, L., & Guedes, C. S. (2013). Lyapunov and Hurwitz based controls for input-output linearisation applied to nonlinear vessel steering. *Ocean Engineering*, 66, 58-68. doi:10.1016/j.oceaneng.2013.04.002
- Rohitha, P. D., Senadheera, S., & Pieper, J. K. (2005). *Fully automated PID and lead/lag compensator design tool for industrial use* (pp. 1009-1014). In Proceedings of the 2005 IEEE Conference on Control Applications. Toronto, Canada. doi:10.1109/CCA.2005.1507262
- Saeed, R. (2012). Nonlinear closed loop optimal control: A modified state-dependent Riccati equation. *ISA transactions*, 52(2), 285-290. doi:10.1016/j.isatra.2012.10.005
- Sun, J., Wang, R., Kang, Y., Miao, K., & Hua, D. (2017). *Application of genetic algorithm and neural network in ship's heading pid tracking control*. In Proceedings of the International Conference on Mechatronics and Intelligent Robotics 2017. Springer, Cham. doi:10.1007/978-3-319-70990-1\_64
- Thomsen, J., Blanke, M., Reid, R. E., & Youhanaie, M. J. S. (2014). *The impact of analog and bang-bang steering gear control on ship's fuel economy*. In Proceedings of the 4<sup>th</sup>

- International Symposium on Ship Operation Autpotation. Genova. doi: 10.13140/2.1.1869.0562
- Tomera, M. (2014). Ant colony optimization algorithm applied to ship steering control. *Procedia Computer Science*, 35, 83-92. doi:10.1016/j.procs.2014.08.087
- Tomera, M. (2017). *Fuzzy self-tuning PID controller for a ship autopilot* (pp. 93-103). In Proceedings of the 12<sup>th</sup> International Conference on Marine Navigation and Safety of Sea Transportation. Gdynia, Poland. doi :10.1201/9781315099132-15
- Tzeng, C. Y., Goodwin, G., & Crisafulli, S. (1999). Feedback linearization design of a ship steering autopilot with saturating and slew rate limiting actuator. *International Journal of Adaptive Control and Signal Processing*, 13, 23-30. doi:10.1002/(SICI)1099-1115(199902)13:1<23::AID-ACS532>3.0.CO;2-E
- Velagic, J., & Vukić, Z. (2004). *The improving of neural network capabilities in on-line identification and tracking control of ship* (pp. 1-6). In Proceedings of the IEEE International Conference on Methods and Models in Automation and Robotics. Miedzyzdroje, Poland.
- Velagic, J., Vukić, Z., & Omerdic, E. (2003). Adaptive fuzzy ship autopilot for track-keeping. *Control Engineering Practice*, 11(4), 433-443. doi:10.1016/S0967-0661(02)00009-6
- Wang, C. X., Liu, J. H., Shen, H. H., & Dai, M. J. (2009). *Design of a lag-lead compensator for the photo-electric platform servo system based on MATLAB*. Retrieved from <http://www.xjishu.com/en/111/y621340.html>
- Wen, Y., Tao, W., Zhu, M., Zhou, J., & Xiao, C. (2020). Characteristic model-based path following controller design for the unmanned surface vessel. *Applied Ocean Research*, 101, 102293. doi:10.1016/j.apor.2020.102293
- Witkowska, A., & Smierzchalski, R. (2007). The use of backstepping method to ship course controller. *International Journal on Marine Navigation and Safety of Sea Transportation*, 1(3), 313-317.
- Witkowska, A., & Smierzchalski, R. (2009). Nonlinear backstepping ship course controller. *International Journal of Automation and Computing*, 6(3), 277-284. doi:10.1007/s11633-009-0277-2
- Witkowska, A., Tomera, M., & Smierzchalski, R. (2007). A backstepping approach to ship course control. *Applied Mathematics and Computer Science*, 17, 73-85. doi:10.2478/v10006-007-0007-2
- Yang, S., Wang, H., Liu, J., Cai, H., & Cao, B. (2011). *Study of efficient ship heading controller* (pp. 4991-4994). In Proceedings of the 2011 International Conference on Electrical and Control Engineering. Yichang, China. doi:10.1109/ICECENG.2011.6058102
- Zhan, Y. L. (2003). The study on neural network control of self-adjusted PID parameters for ship maneuvering. *Ship Science and Technology*, 25(5), 20-23. doi:CNKI:SUN:JCKX.0.2003-05-006.
- Zhang, G., & Zhang, X. (2014). Concise robust adaptive path-following control of underactuated ships using DSC and MLP. *IEEE Journal of Oceanic Engineering*, 39, 685-694. doi:10.1109/JOE.2013.2280822
- Zhang, X. K., Wang X. P., & Zhu, L. (2008). Further thinking on Nomoto model for ships. *Journal of Marine Technology*, 30(2), 2-4. doi:CNKI:SUN:HHJS.0.2008-02-002
- Zhang, X., Han, X., Guan, W., & Zhang, G. (2019). Improvement of integrator backstepping control for ships with concise robust control and nonlinear decoration. *Ocean Engineering*, 189, 106349. doi:10.1016/j.oceaneng.2019.106349